Sustainable Chemistry and Pharmacy 25 (2022) 100598

Contents lists available at ScienceDirect

Sustainable Chemistry and Pharmacy

journal homepage: www.elsevier.com/locate/scp

Green synthesis of highly stable zero-valent iron nanoparticles for organic dye treatment using Cleistocalyx operculatus leaf extract

Nguyen Thi Le [a], Trung-Dung Dang [a,**], Khuat Hoang Binh [b], Tuong Manh Nguyen [b], Truong Nguyen Xuan [a], Duong Duc La [b,***], Ashok Kumar Nadda [c], S. Woong Chang [d], D. Duc Nguyen [d,e,*]

[a] School of Chemical Engineering, Hanoi University of Science and Technology, 1 Dai Co Viet, Ha Noi City, Vietnam
[b] Institute of Chemistry and Materials, Nghia Do, Cau Giay, Ha Noi City, Vietnam
[c] Department of Biotechnology and Bioinformatics, Jaypee University of Information Technology, Waknaghat, Solan, 173234, Himachal Pradesh, India
[d] Department of Environmental Energy Engineering, Kyonggi University, South Korea
[e] Faculty of Environmental and Food Engineering, Nguyen Tat Thanh University, 300A Nguyen Tat Thanh, District 4, Ho Chi Minh City, 755414, Vietnam

ARTICLE INFO

Keywords:
Zero-valent iron
Cleistocalyx operculatus leaf Extract
Green synthesis
Rhodamine B removal

ABSTRACT

Zero-valent iron nanoparticles are considered promising nanomaterials for wastewater treatment. However, the use of highly toxic and expensive chemicals such as sodium borohydride during synthesis has significantly limited the broad application of zero-valent iron. In this study, zero-valent iron nanoparticles (nZVI) were facilely and friendly synthesized using *Cleistocalyx operculatus* leaf extract as a reducing agent. The morphology and structure of the as-prepared nanomaterials were characterized using scanning electron microscopy (SEM), X-ray diffraction (XRD), and Fourier transform infrared spectroscopy (FTIR) analysis. The obtained product was spherical with an average diameter of approximately 100 nm. The prepared nZVI exhibited remarkably stable stability, which remained in the nZVI form for more than one month in open air. The removal efficiency of rhodamine B (RhB) by nZVI reached over 95% in 30 min, proving that the nZVI nanomaterials exhibited a high and quick degradation performance toward RhB. The RhB removal efficiency of nZVI, which was proportional to the amount of nZVI and influenced by pH conditions, was determined using the visible ultraviolet absorption spectroscopy.

1. Introduction

The research and development of nanomaterials have been growing rapidly worldwide in the last few decades owing to their versatile applicability in many industrial fields (Baer et al., 2008; Lines, 2008). Their utilization mostly contributes to molecular sensor engineering (Alcantara et al., 2016; Yola et al., 2015), nanoelectromechanical systems (NEMS) (Guisbiers and Buchaillot, 2008; Voigt et al., 2007), microbiological engineering (Dykmana and Khlebtsov, 2012; Salata, 2004; Thanh and Green, 2010; Xu and Sun, 2013), and the food industry (Bradley et al., 2011; Duncan, 2011). In recent years, the application of nanomaterials in environmental

* Corresponding author.
** Corresponding author.
*** Corresponding author.
E-mail addresses: dung.dangtrung@hust.edu.vn (T.-D. Dang), duc.duong.la@gmail.com (D.D. La), nguyensyduc@gmail.com (D.D. Nguyen).

https://doi.org/10.1016/j.scp.2022.100598
Received 18 August 2021; Received in revised form 29 December 2021; Accepted 3 January 2022
Available online 7 January 2022

treatment and remediation has received significant attention, especially the use of zero-valent iron nanoparticles (nZVI) (Stefaniuk et al., 2016; Lye et al., 2020; Rosales et al., 2012; Zhao et al., 2018). Iron nanomaterials can be used to remove a wide range of contaminants, such as Tetracycline (Lye et al., 2020); NO gas (Rosales et al., 2012); organic compounds (Zhao et al., 2018); chlorinated organic solvents (Huber, 2005; Mukherjee et al., 2016); organic dyes and pigments (Chen et al., 2011; Guo et al., 2015; Hou et al., 2011; Ravikumar et al., 2016); inorganic compounds (Alowitz and Scherer, 2002; Cao et al., 2005); and heavy metal ions (As(III) (Kanel et al., 2005), Pb(II) (Tamez et al., 2016; Jabeen et al., 2013), Cu(II) (Tamez et al., 2016; Danila et al., 2018), Ni(II) (Danila et al., 2018), and Cr(VI) (Zhou et al., 2020)). nZVI is commonly fabricated using various methods such as physical, mechanical, and electrochemical processes; however, chemical techniques are one of the most promising approaches because the techniques can synthesize a large number of iron nanoparticles within a short time, and still ensure uniformity in particle size (Elliott and Zhang, 2001; Zhang et al., 1998). Iron nanomaterials can be formed by chemically reducing iron salts (either organic or inorganic) or iron oxides using a mixture of reductants. One of the most common reductants is sodium borohydride ($NaBH_4$), which is strong enough to reduce ferric iron (Fe(II)) or ferrous iron (Fe(III)) ions to Fe (0) in aqueous media (Yuvakkumar et al., 2011). However, sodium borohydride is considered highly toxic and can cause severe effects on ecosystem and human health. Furthermore, the use of sodium borohydride for nZVI synthesis is relatively expensive. Therefore, green and cheap reductants must be developed to synthesize ZVI nanoparticles (Devatha et al., 2016; Machado et al., 2013) and other nanoparticles (Pachaiappan et al., 2021; Verma and Basheer Khan, 2021).

Recently, many extracts from plants and leaves of *Ficus carica* dried fruit (Demirezen et al., 2019), *Citrus maxima* peel aqueous (Weia et al., 2016), *Eucalyptus* (Martínez-Cabanas et al., 2016), *Avicennia marina* flower (Karpagavinayagam and Vedi, 2019), and green tea (Mareedu et al., 2021) have been successfully used as green reductants for the synthesis of nZVI. The replacement of chemical reductants with plant extracts, as reductants, has resulted in a decrease in operational cost and enhancement of nZVI quality, consequently increasing treatment performance. Nonetheless, each plant produces a particular extract with different chemical properties and reducing capability. In addition, the quality of plant extracts depends on regional conditions such as climate and soil factors, which makes the use of this green synthesis for ZVI nanoparticles not yet globally widespread. In Vietnam, green chemistry research has attracted significant attention from the government and scientists because of the tropical climate and diversity of Vietnamese plants. One of the most promising candidates for use as a green reductant is the extract from *Cleistocalyx operculatus* (CE) leaves, a well-known native plant for medicine and beverages, containing a high proportion of reductant contents such as polyphenols, which can be used to reduce Fe ions to zero-valent Fe. To the best of our knowledge, no study has reported the synthesis of zero-valent iron nanoparticles using CE extract as a reductant.

In this study, CE extract was utilized as a reductant to synthesize nZVI from iron salts for the first time. The morphology and structure of the as-prepared material were characterized using scanning electron microscopy (SEM), X-ray diffraction (XRD), energy-dispersive X-ray (EDX) spectroscopy mapping, and Fourier-transform infrared spectroscopy (FTIR). The detailed removal behavior of the prepared nZVI toward organic dyes was investigated. The effects of adsorbent dosage, pH solutions, and treatment time on treatment performance were also studied and discussed.

2. Experimental section

2.1. Materials

Leaves of CE were collected in Ha Tay Province, Vietnam, and identified. The CE leaves were dried and ground in powder form. $FeCl_3$ and ethanol with a purity higher than 99% were purchased from Xilong Chemicals.

2.2. Preparation of I (CE) extract solutions

Dried CE leaves (5 g) were heated and constantly stirred in 30 mL of ethanol at a temperature– of 50–60 °C for 2 h. Thereafter, the mixture was filtered to collect the CE solution with the addition of ethanol to supplement ethanol evaporation during the extraction process. The concentrated CE extract was further diluted with deionized water at a ratio of 1:20 for Fe ion reduction.

2.3. Synthesis of zero-valent iron nanoparticles

The CE extract solution was filled into a burette and dropwise into a 0.005 M $FeCl_3$ solution, and a continuous stream of nitrogen gas was blown into the three-necked flask to expel the air to help maintain an inert atmosphere throughout the synthesis. The mixture was stirred at a speed of 250 rpm, room temperature, neutral environment, and inert conditions throughout the synthesis process. The ZVI nanoparticles obtained from different concentration ratios of $FeCl_3$/CE extract were 2/1, 1/1, 1/1.5, 1/2, 1/2.5, 1/3, 1/4, 1/5, 1/6, and 1/7. When the CE extract solution was used up, the mixture was agitated for 15 min. The as-prepared nZVI was then immediately added to the RhB solution for dye removal. The nZVI-containing suspension (5 mL) was used to treat 10 mL of 10 ppm RhB solution for 30 min. After treatment, the treated RhB solution was collected via centrifugation (Centrifuge 80-2B) and measured using UV-vis analysis (Agilent 8453 device) to determine the removal percentage. The characteristic wavelength of RhB was 554 nm.

The iron nanoparticles were collected via centrifugation (Centrifuge 80-2B) for morphology and structure analysis and thoroughly washed with absolute ethanol five times. Afterward, the material was dried in a vacuum dryer at approximately 60 °C and used for characterization.

2.4. Treatment process for the removal of rhodamine B

The nZVI materials were evaluated for their ability to be treated with the RhB solution dye. The studies were carried out at ambient temperature, neutral pH, with mild stirring (250 rpm), and a treatment time of 30 min. After treatment, the treated RhB solution was collected via centrifugation (Centrifuge 80-2B) at a speed of 3000 rpm for 5 min and measured via UV-vis analysis (Agilent 8453

device) to determine the removal percentage. The characteristic wavelength of RhB was 554 nm.

2.5. Effect of the nZVI dosage on the removal performance of RhB

Various nZVI suspensions (0.5, 1, 1.5, 2, and 2.5 mL) were added to 10 mL of 10 ppm RhB solution to evaluate the effect of the amount of nZVI on RhB removal efficiency. The treatment time was 30 min. The experiment was carried out at room temperature and neutral pH, with mild stirring (250 rpm). The treated RhB dye was measured via UV-Vis analysis at 554 nm.

2.6. Effect of treatment time on the removal performance of RhB

To evaluate the effect of treatment time on the removal efficiency of RhB, 5 mL of nZVI suspension was added to 10 mL of 10 ppm RhB solution with mild stirring (250 rpm) for various times: 1/3, 2/3, 1, 3, 5, 10, and 30 min.

2.7. Effect of the RhB concentration and pH on the removal performance of RhB

To evaluate the effect of treatment time on the removal efficiency of RhB, 5 mL of nZVI suspension was introduced into 10 mL of RhB solution with different concentrations (1, 5, 10, 15, and 20 ppm), with mild stirring for 30 min.

To evaluate the effect of treatment pH on the RhB removal efficiency, 10 mL of 10 ppm RhB solution with different pH of 1, 3, 5, 7, 9, and 11 were treated with 5 mL of nZVI, with mild stirring for 30 min. The solution pH was measured using the portable pH monitor (Hanna HI98127), adjusting the pH of solution RhB dye with HCl 1 M and NaOH 1 M solutions and pH = 7.01 Hanna HI7007L/1L standard solution.

2.8. Effect of CE extract on the removal performance of RhB

To demonstrate that the CE extract did not participate in the removal of RhB, 5 mL of CE extract was added to 10 mL of 10 ppm RhB with a processing time of 30 min.

3. Results and discussion

3.1. Green synthesis of ZVI nanoparticles and their characterizations

The synthesis process of nZVI using CE extract is depicted in Fig. 1. Briefly, $FeCl_3$ was transferred to a three-neck flask under inert conditions using nitrogen gas (N_2), while the CE extract solution was gradually added to $FeCl_3$ at a rate of 4s per drop. The effect of the optimized CE extract content for nZVI synthesis on the removal performance of the prepared nZVI toward RhB organic dyes was evaluated, as shown in Fig. 2. It is evident from the Figure that when the CE content increased, the removal percentage of RhB increased and reached a maximum of approximately 100% at the Fe(III)/CE extract ratio of approximately 1/3. The concentration of nZVI nanoparticles in the suspension was determined to be approximately 0.07 g/L. This result demonstrates that at this ratio between Fe(III) ions and CE extract, the highest amount of nZVI was obtained. Thus, an Fe(III)/CE ratio of 1/3 was selected for the synthesis of nZVI nanoparticles for further studies.

A further increase in the CE content led to a decrease in the removal efficiency of RhB. This phenomenon could be explained by the fact that when the CE content increased, the amount of surfactant or other organic compounds in the extract, which covered the surface

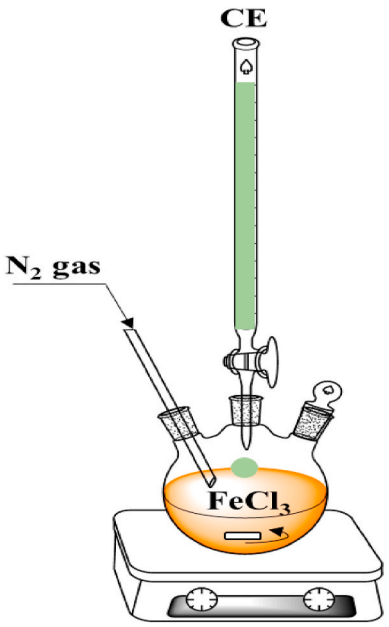

Fig. 1. Synthesis diagram of nZVI from CE extract and $FeCl_3$ 0.005 M solution.

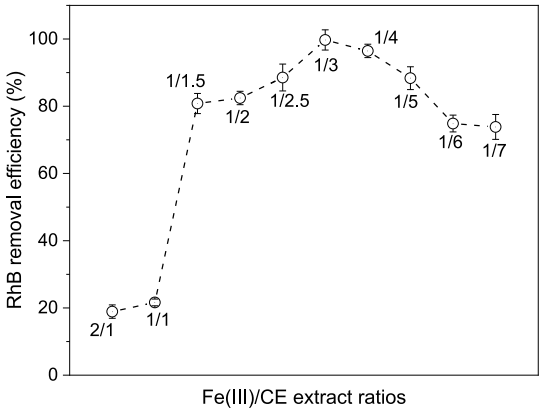

Fig. 2. Effect of the Fe(III)/CE extract ratios on the 10 ppm RhB removal efficiency.

of the newly formed nZVI, increased, thus decreasing the reactivity of nZVI toward RhB. Additionally, the reaction of nZVI with other organic compounds in the CE extract could also be a reason for the decline in the RhB removal efficiency.

The morphology of the as-prepared nZVI nanoparticles was observed using scanning electron microscopy (SEM), as shown in Fig. 3. It can be clearly seen that the resultant nZVI has a spherical structure with a diameter ranging from 30 to 300 nm, because the particles are in nanoscale and have a high surface charge density, the nZVI nanoparticles tend to aggregate to form nanoclusters.

Fig. 4 shows the XRD pattern of the fabricated nZVI via green synthesis, which was used to determine the crystallinity of the material. The XRD pattern shows two characteristic peaks at approximately 46° and 65° and were assigned to the characteristic peaks of the zero-valent iron (Maamoun et al., 2019; Maamoun et al., 2020). The appearance of other peaks in the XRD pattern was assigned to the iron oxides formed by the oxidization of iron and oxygen during the XRD analysis. These interference peaks were relatively sharp, indicating that the iron oxides were highly crystalline.

The distribution of the elements in the prepared nZVI nanoparticles was investigated using EDX mapping, as shown in Fig. 5. The EDX spectrum clearly indicates that Fe atom with a negligible amount of C and O elements were the major element, which confirms that the prepared nZVI nanoparticles are highly stable because their surfaces were coated with polysaccharide components in the CE extract. The small amounts of C and O are ascribed to the organic components in the CE extract and the partial oxidation of iron by oxygen.

The FTIR spectra of the prepared nZVI nanoparticles are shown in Fig. 6. The strong absorption band at 3446 cm^{-1} is ascribed to the sketching vibration of the O-H bond from moisture or adsorbed water on the surface of the particle. The peak at 1636 cm^{-1} is a characteristics of the C=O bond, which belongs to the aldehyde and ketone groups in the CE extract. The band at 668 cm^{-1} is related to the oscillation of the Fe-O bond on the surface of the nZVI nanoparticles. This indicates the successful formation of nZVI nanoparticles, and the resultant nZVI was covered with a polysaccharide coating from the CE extract.

In a liquid solution, the zeta potential is employed to determine the interaction forces (attraction or electrostatic repulsion) between particles, which is a decisive factor for the stability of the particles in aqueous media. Fig. 7 shows the zeta potential of the nZVI synthesized using the CE extract with an Fe(III)/CE extract ratio of 1:3, at ambient temperature and neutral pH, with mild stirring. The zeta potential value was determined to be around −18.59 mV, indicating that the prepared nZVI is relatively stable in the aqueous environment. This might be that the presence of the capping molecules with the negatively charged groups in the extract contribute to the stability of the nZVI nanoparticles.

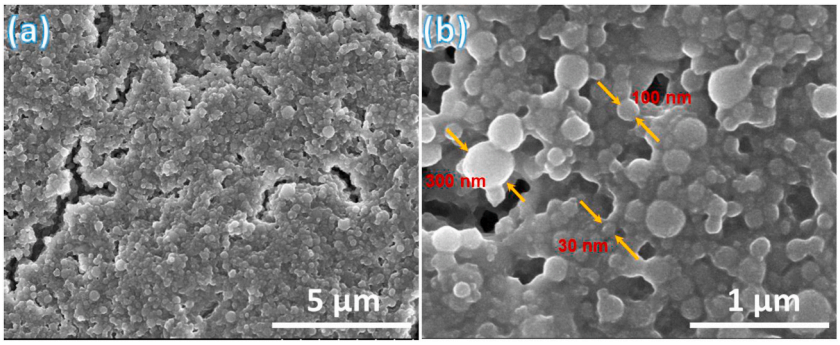

Fig. 3. SEM images of nZVI nanoparticles obtained with Fe(III)/CE extract ratio of 1:3, at ambient temperature and neutral pH, with mild stirring.

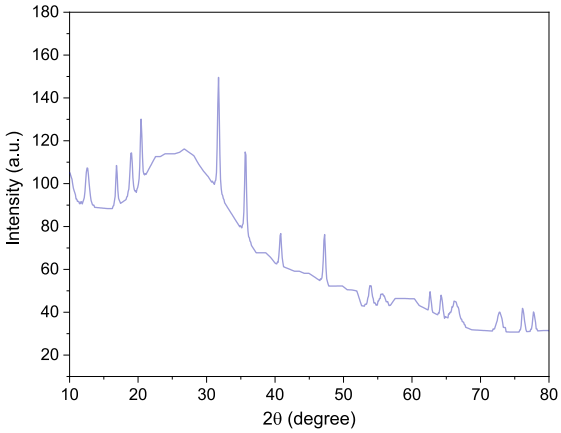

Fig. 4. XRD pattern of nZVI synthesized with Fe(III)/CE extract ratio of 1/3, at ambient temperature and neutral pH, with mild stirring.

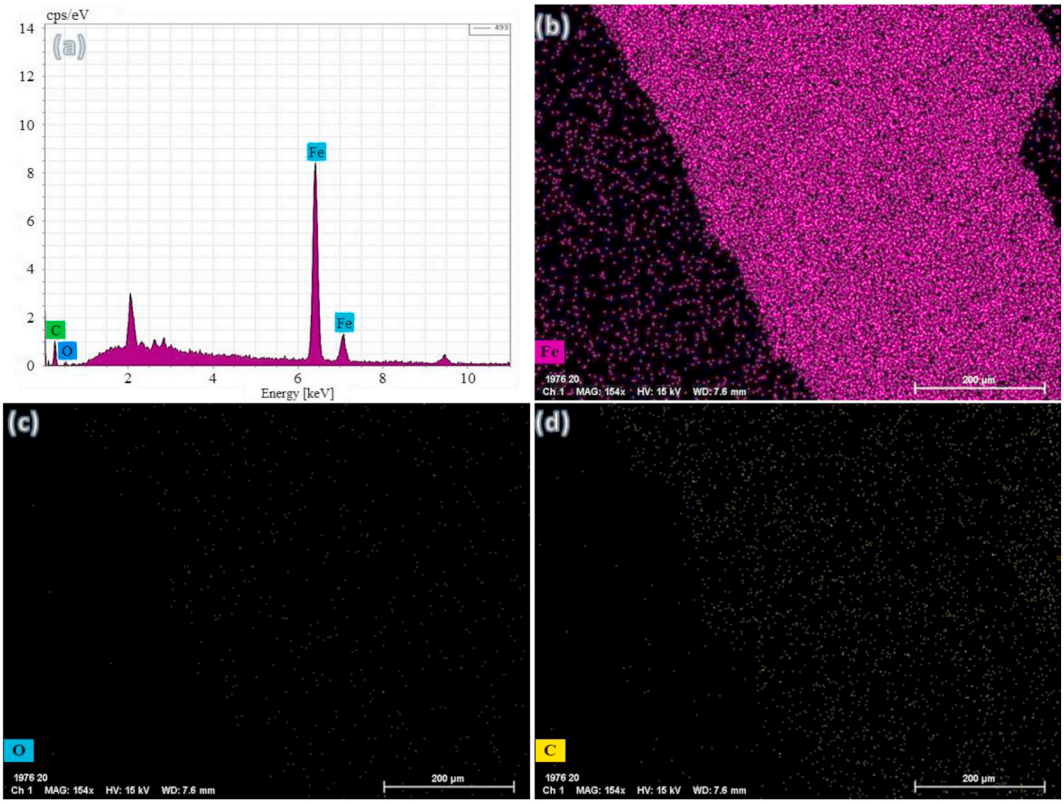

Fig. 5. EDX spectrum and mapping image of nZVI synthesized using the CE extract with ratio Fe(III)/CE extract of 1:3, at ambient temperature and neutral pH, with mild stirring.

3.2. RhB removal performance by nZVI

The level of decrease in the absorption peak at 554 nm was used to calculate the RhB removal performance. The absorption peak intensity of the RhB relatively decreased when the amount of nZVI was raised from 0.5 to 2.5 mL (Fig. 8). The initial absorption peak of 10 ppm RhB was regarded as 100%. When nZVI was gradually added to the RhB dye solution, the absorbance started to decline, indicating the breakdown of bonds in the structure of the RhB molecules. When nZVI-containing suspension (2.5 mL) was added, the absorbance of RhB decreased to 3.4%. The RhB removal efficiency was determined according to Equation one, and the results are presented in Fig. 9. It can be seen that the greater the amount of nZVI added, the higher the efficiency; with 2.5 mL of nZVI, the removal percentage reached 96.61%.

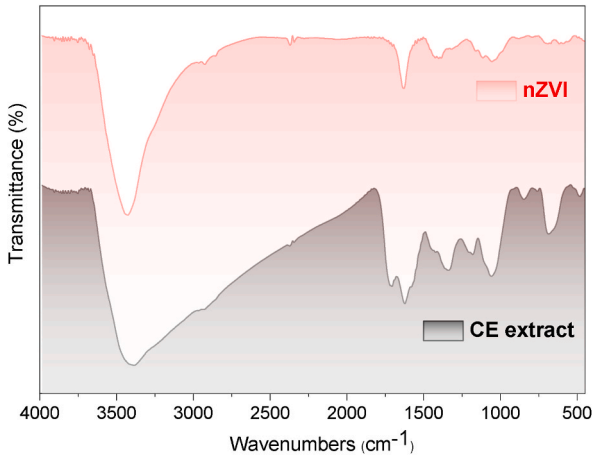

Fig. 6. FTIR spectrum of CE extract and green synthesized nZVI nanoparticles at ambient temperature and neutral pH, with mild stirring. (For interpretation of the references to color in this figure legend, the reader is referred to the Web version of this article.)

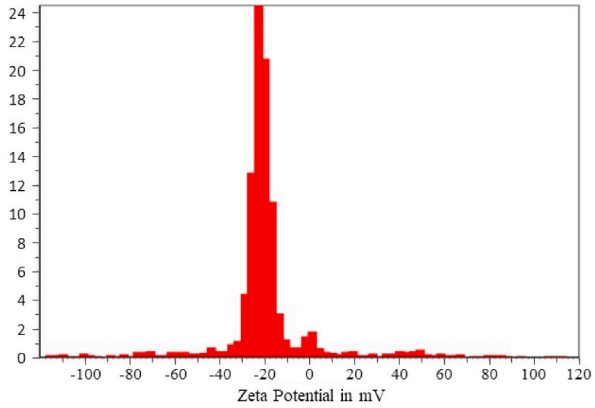

Fig. 7. Zeta potential of the nZVI synthesized using the CE extract with ratio Fe(III)/CE extract of 1:3, at ambient temperature and neutral pH, with mild stirring.

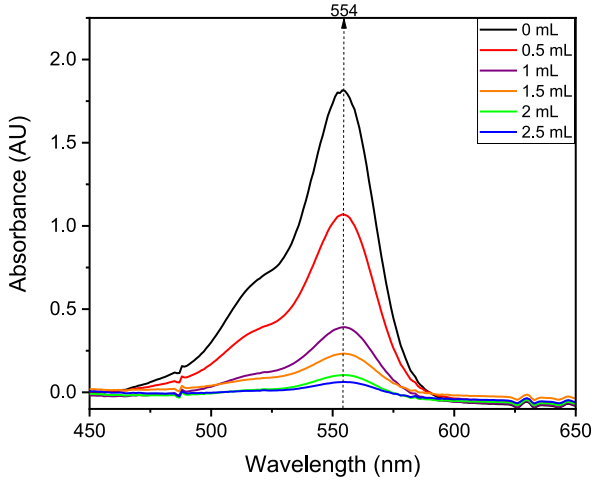

Fig. 8. UV-Vis spectrum of 10 mL of 10 ppm RhB after being treated with different amounts of nZVI at ambient temperature and neutral pH, with mild stirring.

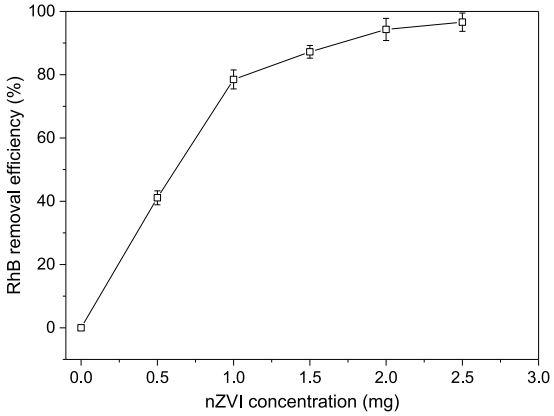

Fig. 9. RhB removal efficiency with different amounts of nZVI at ambient temperature and neutral pH, with mild stirring.

Color removal efficiency = (Ao-An)*100/Ao

where Ao is the initial absorbance of RhB at 554 nm wavelength, and An is the absorbance of RhB at 554 nm wavelength after treatment with different amounts of nZVI.

The treatment time was also an important factor affecting the RhB removal efficiency of nZVI prepared from green synthesis using CE extract. As shown in Fig. 10a, the color degradation of RhB occurred rapidly. Specifically, the removal efficiency reached 84.95% after only 20 s, and after 3 min of treatment time, the removal percentage reached 92%. After 30 min of treatment time, the removal percentage was calculated to be 95%, which is much faster than that of nZVI prepared by Soni et al. (2015). In this study, the highest RhB removal percentage of more than 95% by nZVI was achieved only after 6–8 h under UV light irradiation.

For practical applications, the pH of solution played a significant role in the treatment efficiency of RhB. In this study, the effect of pH on the RhB removal efficiency of nZVI nanoparticles was investigated. HCl or NaOH was used to adjust the pH of solutions to obtain a pH range from 1 to 11 (Fig. 10b). The experiment showed that RhB could be effectively removed by nZVI under a pH ranging from 3 to 7, which is mildly acidic to neutral, and in the strongly acidic pH, iron nanoparticles reacted with H^+ ions and formed the reducing agents for RhB removal. The decrease in the RhB removal performance under strongly alkaline conditions can be attributed to the conversion of the supernatant iron ions into Fe (III) - hydroxide or Fe (III) - oxide membrane, which hinders the reaction of nZVI nanoparticles.

3.3. RhB removal performance by CE extract

The UV-Vis results of the RhB solution treated with CE extract are shown in Fig. 11. The height of the RhB peak did not change significantly, thus proving that the CE extract was not capable of treating the RhB dye. There is a characteristic peak shift of RhB from 554 nm to 570 nm due to the physical mixing of colors between the pink of RhB and the green CE extract.

4. Conclusions

In summary, zero-valent iron nanoparticles were successfully synthesized in a friendly and facile manner using *Cleistocalyx*

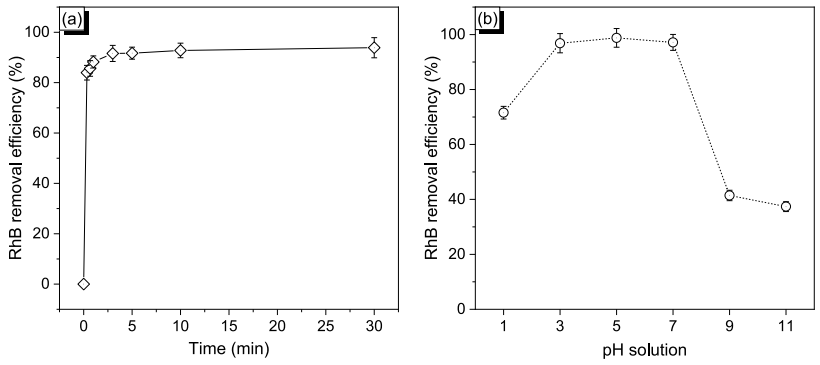

Fig. 10. Effect of treatment time (a) and pH of solution (b) on 10 ppm RhB removal efficiency of nZVI nanoparticles at ambient temperature, with mild stirring.

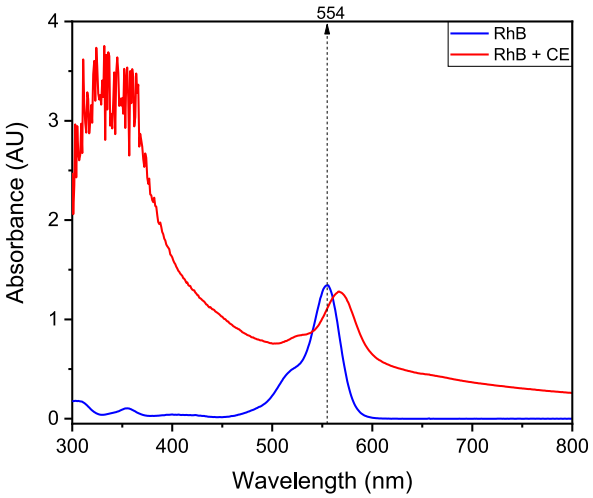

Fig. 11. UV-Vis spectrum of 10 mL of RhB 10 ppm before and after treatment with 5 mL CE extract at ambient temperature and neutral pH, with mild stirring.

operculatus leaf extract with an Fe(III)/CE extract ratio of 1/3. The prepared nZVI nanoparticles were spherical with an average diameter of approximately 100 nm. Unlike nZVI prepared via the conventional approach using a strong reductant, the nZVI nanoparticles obtained via the CE extract reductant were highly stable under the surrounding conditions, which is attributed to the formation of a thin organic coating on the surface of the newly prepared nZVI. The obtained nZVI nanomaterial showed quick and high removal efficiency toward RhB, with a treatment percentage of up to 95% only after 30 min of treatment time at an RhB concentration of 10 ppm. As the amount of nZVI increased, the treatment efficiency increased, and the optimal solution pH for the treatment of RhB with nZVI was in the pH range of 3–7. With this high removal efficiency, and especially the safe and quick treatment of RhB or other organic dyes, the nZVI prepared from CE extracts is considered a promising material for treating dye-containing industrial wastewater in practical applications. nZVI nanoparticles for the treatment of practical industrial wastewater will be evaluated in further studies.

Author contribution statement

Le Nguyen Thi, Conceptualization, Writing - original draft. Trung-Dung Dang Supervision, Methodology, Data curation, Formal analysis. Hoang Binh Khuat Methodology, Writing - review & editing. Tuong Manh Nguyen Data curation, Formal analysis, Writing - review & editing. Truong Nguyen Xuan Methodology, Formal analysis, Duong Duc La Conceptualization, Supervision, Methodology, Writing - review & editing. Ashok Nadda Conceptualization, Writing - review & editing. S. Woong Chang Resources, Writing - review & editing. D. Duc Nguyen Conceptualization, Supervision, Project administration, Writing - review & editing.

Declaration of competing interest

The authors declare that they have no known competing financial interests or personal relationships that could have appeared to influence the work reported in this paper.

References

Alcantara, D., Lopez, S., García-Martin, M.L., Pozo, D., 2016. Nanomed. Nanotechnol. Biol. Med. 12, 1253–1262.
Alowitz, M., Scherer, M., 2002. Environ. Sci. Technol. 36, 299–306.
Baer, D.R., Amonette, E., Engelhard, M.H., Gaspar, D.J., Karakoti, A.S., Kuchibhatla, S., Nachimuthu, P., Nurmi, J.T., Qiang, Y., Sarathy, V., Seal, S., Sharma, A., Tratnyeke, P.G., Wanga, C.-M., 2008. Surf. Interface Anal. 40, 529–537.
Bradley, E.L., Castle, L., Chaudhry, Q., 2011. Trends Food Sci. Technol. 22, 604–610.
Cao, J., Elliott, D., Zhang, W.-x., 2005. J. Nanoparticle Res. 7, 499–506.
Chen, Z.-x., Jin, X.-y., Chen, Z., Megharaj, M., Naidu, R., 2011. J. Colloid Interface Sci. 363, 601–607.
Danila, V., Vasarevicius, S., Valskys, V., 2018. Energy Proc. 147, 214–219.
Demirezen, D.A., Yıldız, Y.S., Yılmaz, S., Yılmaz, D.D., 2019. J. Biosci. Bioeng. 127, 241–245.
Devatha, C.P., Thalia, A.K., Katte, S.Y., 2016. J. Clean. Prod. 139, 1425–1435.
Duncan, T.V., 2011. J. Colloid Interface Sci. 363, 1–24.
Dykmana, L., Khlebtsov, N., 2012. Chem. Soc. Rev. 41, 2256–2282.
Elliott, D.W., Zhang, W.-X., 2001. Environ. Sci. Technol. 35, 4922–4926.
Guisbiers, G., Buchaillot, L., 2008. J. Phys. Appl. Phys. 41, 172001.
Guo, W., Hao, F., Yue, X., Liu, Z., Zhang, Q., Li, X., Wei, J., 2015. Environ. Prog. Sustain. Energy 35, 48–55.
Hou, M.-F., Liao, L., Zhang, W.-D., Tang, X.-Y., Wan, H.-F., Yin, G.-C., 2011. Chemosphere 83, 1279–1283.
Huber, D.L., 2005. Small 5, 482–501.
Jabeen, H., Kemp, K.C., Chandra, V., 2013. J. Environ. Manag. 130, 429–435.
Kanel, S.R., Manning, B., Charlet, L., Choi, H., 2005. Environ. Sci. Technol. 39, 1291–1298.
Karpagavinayagam, P., Vedi, C., 2019. Vacuum 160, 286–292.
Lines, M.G., 2008. J. Alloys Compd. 449, 242–245.
Lye, J.W.P., Saman, N., Noor, A.M.M., Mohtar, S.S., Othman, N.S., Sharuddin, S.S.N., Kong, H., Mat, H., 2020. Chem. Eng. Technol. 43 (7), 1285–1296.

Maamoun, I., Eljamal, O., Falyouna, O., Eljamal, R., Sugihara, Y., 2019. Water Sci. Technol. 80, 1996–2002.Maamoun et al., 2020 Maamoun, Ibrahim, Eljamal, Osama, Eljamal, Ramadan, Falyouna, Omar, Sugihara, Yuji, 2020. Appl. Surf. Sci. 506, 145018.
Machado, S., Pinto, S.L., Grosso, J.P., Nouws, H.P.A., Albergaria, J.T., Delerue-Matos, C., 2013. Sci. Total Environ. 445, 1–8.
Mareedu, T., Poiba, V., Vangalapati, M., 2021. Mater. Today Proc. 42, 1498–1501.
Martínez-Cabanas, M., López-García, M., Barriada, J.L., Herrero, R., Vicente, M.E. S.d., 2016. Chem. Eng. J. 301, 83–91.
Mukherjee, R., Kumar, R., Sinha, A., Lama, Y., Saha, A.K., 2016. Crit. Rev. Environ. Sci. Technol. 46, 443–466.
Pachaiappan, R., Rajendran, S., Ramalingam, G., Vo, D.-V.N., Priya, P.M., Soto-Moscoso, M., 2021. Chem. Eng. Technol. 44, 551–558.
Ravikumar, K.V.G., Dubey, S., pulimi, M., Chandrasekaran, N., Mukherjee, A., 2016. J. Mol. Liq. 224, 589–598.
Rosales, E., Pazos, M., Sanroman, M.A., 2012. Chem. Eng. Technol. 35 (4), 609–617.
Salata, O., 2004. J. Nanobiotechnol. 2, 1–6.
Soni, H., Kumar, J.I.N., Patel, K., Kumar, R.N., 2015. Indian J. Nanosci. 3, 1–6.
Stefaniuk, M., Oleszczuk, P., Ok, Y.S., 2016. Chem. Eng. J. 287, 618–632.
Tamez, C., Hernandez, R., Parsons, J.G., 2016. Microchem. J. 125, 97–104.
Thanh, N.T.K., Green, L.A.W., 2010. Nano Today 5, 213–230.
Verma, R., Basheer Khan, A., 2021. Chem. Eng. Technol. 44, 819–825.
Voigt, A., Heinrich, M., Martin, C., Llobera, A., Gruetzner, G., Peŕez-Murano, F., 2007. Microelectron. Eng. 84, 1075–1079.
Weia, Y., Fang, Z., Zheng, L., Tana, L., Tsang, E.P., 2016. Mater. Lett. 185, 384–386.
Xu, C., Sun, S., 2013. Adv. Drug Deliv. Rev. 65, 732–743.
Yola, M.L., Eren, T., Atar, N., 2015. Sensor. Actuator. B 210, 149–157.
Yuvakkumar, R., Elango, V., Rạendran, V., Kannan, N., 2011. Digest J. Nanomater. Biostruct. 6, 1771–1776.
Zhang, W.-x., Wang, C.-B., Lien, H.-L., 1998. Catal. Today 40, 387–395.
Zhao, Y., Han, Y., Zhao, Z., 2018. Chem. Eng. Technol. 41 (11), 2203–2211.
Zhou, N., Gong, Kedong, Hu, Qian, Cheng, Xiang, Zhou, Juying, Dong, Mengyao, Wang, Ning, Ding, Tao, Qju, Bin, Guo, Zhanhu, 2020. Chemosphere 242, 125235.